PCCP

Accepted Manuscript

ROYAL SOCIETY OF CHEMISTRY

www.rsc.org/pccp

Journal Name

ARTICLE

Water-Assisted Self-Photoredox of 2-(1-Hydroxyethyl)-9,10-Anthraquinone Through a Triplet Excited State Intra-Molecular Proton Transfer Pathway

Received 00th January 20xx,
Accepted 00th January 20xx

DOI: 10.1039/x0xx00000x

www.rsc.org/

Jingze Dai,[a] Juan Han,[a] Xuebo Chen,*[a] Weihai Fang,[a] Jiani Ma,[b] and David Lee Phillips*[c]

Using multi-configurational perturbation theory (CASPT2//CASSCF), a novel self-photoredox reaction for 2-(1-hydroxyethyl)-9,10-anthraquinone was proposed to effectively occur through two steps of triplet excited state intra-molecular proton transfer (ESIPT) reaction aided by water wires without the introduction of an external oxidant or reductant. The photoinduced charge transfer along the desired direction was determined to be the major driving force for the occurrence of the energetically favorable ESIPT in the triplet state, in which the water wires function as an effective proton relay and photocatalyst to lower the reaction barrier. The computational results provide convincing evidence that the deprotonation of the hydroxyl group in the triplet state and connecting water molecule(s) between that hydroxyl group and the carbonyl group that is protonated by a nearby water molecule in the water wire is the initial reaction step that triggers the protonation of the carbonyl group seen in the previously reported time-resolved spectroscopy experiments that produces a protonated carbonyl triplet intermediate that then undergoes a subsequent deprotonation of the methylene C-H in the triplet and ground states to complete the self-photoredox reaction of anthraquinone. Comparison of the theoretical results with previously reported results from time-resolved spectroscopy experiments indicate the photoredox reactions can occur either via a concerted or non-concerted deprotonation-protonation of distal sites of the molecule assisted by the connecting water molecules. These new insights will help provide benchmarks to elucidate the photochemistry of the anthraquinone and benzophenone compounds in acidic and/or neutral aqueous solutions.

Introduction

The photochemistry of anthraquinone (AQ) and its derivatives has been extensively investigated[1-21] due to the ability of these compounds to accept electrons and efficiently abstract hydrogen from solvents and other donors,[2-7] as well as their widespread use as photosensitizers, photocatalysts for solar energy processors and photoinitiators for the photopolymerization of various monomers and prepolymers.[8,9] AQ in an aqueous solution is frequently used as a platform for developing photoremovable protecting groups that have great potential for use in chemical and biological applications.[10-13] In the past few decades, a new class of photochemistry of AQs in aqueous solutions has been studied by Wan[22] and Phillips[23] as well as their coworkers. In their studies, a novel photoredox reaction reduces the ketone moiety to its alcohol and the side chain alcohol moiety is simultaneously oxidized to its aldehyde (or ketone) form.[22-23] As an illustrative example, 2-(1-Hydroxyethyl)-9,10-anthraquinone (2-HEAQ; Scheme 1) underwent an efficient intersystem crossing to its triplet excited state [^{3}(2-HEAQ)], and no reaction was observed in an aprotic solvent (acetonitrile).[22(b),23] This confirms the traditionally held thinking that

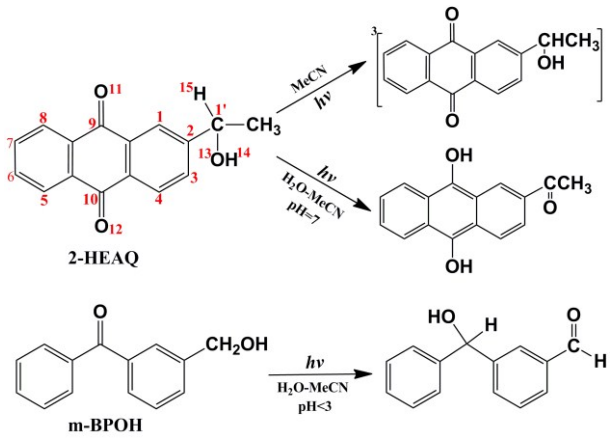

Scheme 1. Water-Assisted Self-Photoredox Reaction in Aqueous Solutions for 2-HEAQ and m-BPOH.

[a] Department of Chemistry, Beijing Normal University, Xin-wai-da-jie 19, Beijing 100875, P. R. China. Email: xuebochen@bnu.edu.cn
[b] College of Chemistry and Materials Science, Northwest University, Xi'an, P. R. China.
[c] Department of Chemistry, The University of Hong Kong Pokfulam Road, Hong Kong, P.R. China. Email: phillips@hku.hk

Electronic Supplementary Information (ESI) available: Figures and Tables as well as Cartesian coordinates.. See DOI:10.1039/x0xx00000x

AQs are primarily used as triplet sensitizers or hydrogen abstractors.[2-7] However, in neutral (pH = 7) aqueous solutions (MeCN:H_2O, 1:1), a highly efficient intramolecular photoredox reaction ($\Phi \approx 0.8$) was observed only in the presence of water with the clean formation of the redox product of 2-acetyl-9,10-dihydroxyanthracene.[22(b),23] Experimental results indicate that water plays an essential role in the photoredox reaction to stabilize the initial excited state and the generated intermediates as well as to provide a source of the required protons in the reaction processes.[23] Consistently, a plausible mechanism of the water-assisted excited state intra-molecular proton transfer (ESIPT) has been proposed to elucidate the self-photoredox reaction mechanism of 3-(hydroxymethyl) benzophenone (m-BPOH) in our previous studies.[24]

Although the structural characteristic of 2-HEAQ embodies noticeable similarity with that of *m*-BPOH, the photoredox reaction conditions are quite different. For example, as shown in Scheme 1, 2-HEAQ undergoes a photoredox reaction in a neutral aqueous solution,[22(b),23] while harsh reaction conditions (pH < 3) are required to trigger the photoredox reaction for *m*-BPOH.[24] This result indicates that the detailed photophysical and photochemical mechanism by which water mediates this self-photoredox reaction has been modified from *m*-BPOH to 2-HEAQ. A quantitative study is required to obtain the mechanistic explanation for these differences and how this novel reaction with 2-HEAQ takes place without the participation of an extra oxidant or reductant. Several intermediates[5,23] and possible pathways[22-23] have been proposed in previous experimental studies to address the photochemistry of AQ compounds under different solvent and excitation wavelength conditions. To further explore the mechanistic details of the water-mediated self-photoredox reaction of AQ compounds we have done a more detailed theoretical investigation of the reaction mechanism that is now reported here. In our previous studies,[24-29] high-level electronic structure calculations provided detailed information on the Frank-Condon (FC) excitation, reactive intermediates, products and the relaxation pathways of various aromatic compounds, which could be compared in a quantitative manner with experimental observations.[30-35] In this study, we employ the same CASPT2//CASSCF computational protocol to describe explicitly the properties of the initial excitation and subsequent relaxation pathways in an effort to unravel the mechanism of the self-photoredox reaction for AQ compounds.

Computational methods

Simulation Model Setup

To mimic the water-assisted ESIPT reaction of 2-HEAQ, water molecules are required to aid the proton transfer between the donors of H14/H15 and acceptors of O12/O11 that are spatially separated by 5.0~7.0 Å distance (see Scheme 1, Figures 2 and 4 for the atom numbering and schematic structures). Numerous test computations were performed using density functional theory (DFT) at the B3lYP/6-31G* level to determine the structural configuration of the 2-HEAQ-water complex that will be employed as the simulation model for the subsequent excited state calculations. The various 2-HEAQ·nH_2O (n=1-6) complexes in their hydrogen bonding and supra-molecular forms underwent optimization and were confirmed to be potential energy minima by harmonic vibrational frequency analysis, respectively. The stabilization energies for each configuration were obtained by calculating the energetic difference between the hydrogen bonding and supra-molecular forms and summarized in Table S1-1 of the Electronic Supporting Information (**ESI**) together with the corresponding schematic structures (see Figure S1-1 in the **ESI**). Computational results show that the stabilization energy gradually increases with the formation of more hydrogen bonds between the water molecules and the 2-HEAQ molecule. However, the introduction of extra H_2O molecules does not cause a significant change in the stabilization energy when both the ESIPT donor (H15/H14) and the acceptor (O11/O12) have been saturated by the minimum number of water molecules i.e. 2 for O11…H15 and 3 for O12…H14. The presence of additional water molecules is only able to enlarge the magnitude of the water wires but imposes a negligible influence on the strength of the hydrogen bonds that always remain in the range of 1.80~2.00 Å. This distance is long enough to aid the facilitation of the ESPIT reaction between the water wires and 2-HEAQ. Hence, the structural configuration with the minimum number of water molecules, i.e., 2-HEAQ·5H_2O was employed as the starting simulation model, which significantly reduces the computational cost while this does not lead to the fundamental discrepancy in the mechanistic understanding of the ESIPT reaction on the other hand. Similar selection strategies have been successfully applied to the water-assisted ESIPT reactions for benzophenone (BP)[24] and ketoprofen (KP)[26] compounds as well as in some protein systems[36] in our previous studies. To examine the role of acetonitrile, the optimization attempts have been performed by using five water molecules and one acetonitrile solute with 2-HEAQ. It was found that acetonitrile is always squeezed out of the water wire, surrounding one water molecule via one single H-N hydrogen bond. This indicates that acetonitrile is unlikely to take part in the proton transfer process and might be serving as a bulk solvent only. This is in good agreement with the traditionally held thinking that acetonitrile is a good proton acceptor but not an ideal donor. Consistently, no photoredox reaction was observed in neat acetonitrile solvent[22,23] and isotopic experiments suggested that proton arises from water, not from acetonitrile.[30(b)]

Minimum Energy Profiles Mapping

The *ab initio* calculations were primarily performed at the complete active space self-consistent field (CASSCF)[37,38] level of theory with a total of 12 electrons in 10 active space orbitals (12e/10o) with the 6-31G* basis set, and this level of theory is referred to as CASSCF(12e/10o)/6-31G*. To describe the processes of the water-assisted self-photoredox of 2-HEAQ, σ/σ* orbitals of O13-H14 and the n orbital of O12 were included in the active space to account for the first step of ESIPT between the 1'-substituted hydroxyl (O13-H14) and the carbonyl C10=O12 of 2-HEAQ·5H_2O. These three orbitals were replaced by σ/σ* orbitals of C1'-H15 and the n orbital of O11 when the second step of the reaction was calculated for the ESIPT between methylene C1'-H15 and the carbonyl C9=O11. The rest of the 8e/7o active orbitals originate from high-lying occupied π and low-lying π* orbitals, which can be used to describe the different electron transitions from the right/left chromophores to the central anthraquinone ring. All of these orbitals in the active space

for the CASPT2//CASSCF(12e/10o) calculations are schematically shown in Figures S1-2 and S1-3. To inspect the basis set effects on the optimized geometries and their excitation energies, some critical points, i.e., the minima, the transition states and the intermediates were re-optimized at the CASSCF(12e/10o)/6-31G** level of theory by adding the polarization functions to the hydrogen atoms. To inspect the role of the water molecules from a theoretical perspective, all of the stationary structures (reactants, products and transition states) were optimized on the first ESIPT reaction in the T_{RCT2} state pathway for the isolated 2-HEAQ (without water molecules) at the CASSCF(12e/10o)/6-31G**(gas phase) and also at the CASSCF(12e/10o)/6-31G**/PCM (water solvent) levels of theory.

All of the minima in the singlet excited state were obtained by a full system state-averaged CASSCF optimizations[39] using a two-root equally weighted (0.5:0.5) approach whereas a single root optimization was adopted in the triplet and ground states. The same state-averaged method was employed to determine the geometry of the intersection space of the two electronic states with the same spin multiplicity and the minimum-energy crossing points between the singlet and triplet states were optimized using Slater determinants. The transition state (TS) in the triplet state was determined by the conventional TS optimization, which was further confirmed to be the saddle point at the reduced active space and basis set, i.e., CASSCF(10e/8o)/6-31G. The minimum energy profiles (MEPs) were mapped by intrinsic reaction coordinate (IRC) computations[40,41] at the CASSCF(12e/10o)/6-31G* level of theory to connect these critical points in several possible excited and ground states. The ESIPT paths in the triplet state were successively plotted starting from the TS(T_{RCT2}) in the first step of the reaction or the singlet-triplet crossing [STC(T_{RCT2}/S_0)] in the second one by a numerical gradient calculations along the direction given by the IRC equation.[40,41] The STC(T_{RCT2}/S_0) was also taken as the starting point to drive the IRC calculations in the ground state proton transfer reaction.

To consider the dynamic electron correlation effects, the single-point energy of the optimized geometries in these IRC computations was recalculated at the second-order perturbation method (CASPT2)[42,43] level of theory using a five-root state-averaged CASSCF zeroth-order wave function. Therefore, the MEPs of 2-HEAQ·5H_2O were computed at the CASPT2//IRC/CASSCF(12e/10o)/6-31G* level of theory along the unbiased reaction coordinates to gain insight into how this fundamentally important reaction occurs in an aqueous solution. The vertical/adiabatic excitation energies were obtained by CASPT2//CASSCF(12e/10o)/6-31G*, 6-31G** computations based on the CASSCF optimized structures. The calculated values are very close to the experimental data due to the comprehensive treatment of the electron correlation effects. In this work, all of the DFT and CASSCF calculations, together with the IRC pathway calculations, were performed using the Gaussian program package,[44] whereas the CASPT2 computations were carried out with the Molcas program package.[45]

Results and discussion

Vertical Excitation of 2-HEAQ·5H_2O

Table 1 summarizes the vertical excitation energies (ΔE, kcal/mol), oscillator strengths (*f*), and dipole moments (DM, Debye) of the different transitions for the 2-HEAQ·5H_2O complex as well as the assignment of the excited-state character. As shown in Table 1, a pair of "bright" spectroscopic states have been found for 2-HEAQ·5H_2O with the same magnitude of the oscillator strength (0.35-0.36) that are 5~900 times larger than those of other transitions. The electronic population indicates that the unpaired electrons are distributed in the 1-phenylethanol moiety and the central anthraquinone ring, particularly in the carbonyl groups of C9=O11/C10=O12. This result indicates that the two bright state transitions exhibit charge transfer (CT) character originating from one electron promotion of the right chromophore (1-phenylethanol) π orbital to the π* orbital of the two C=O groups and are referred to as $S_{RCT1}(^1\pi\pi^*)$ and $S_{RCT2}(^1\pi\pi^*)$. The $S_0\rightarrow S_{RCT1}(^1\pi\pi^*)$ /$S_0\rightarrow S_{RCT2}(^1\pi\pi^*)$ FC excitations result in excessive negative charges of 0.0587/0.0533 and 0.0593/0.0564 around O11 and O12, respectively, compared to the ground state charges. These accumulated negative charges are considerably lower than those in KP (0.35)[26] and *o*-acetylphenylacetic acid (0.5)[25] upon FC excitation in the bright excited state in our previous studies. This indicates that $S_{RCT1}(^1\pi\pi^*)$ and $S_{RCT2}(^1\pi\pi^*)$ are unlikely to serve as the ideal precursor states for the subsequent ESIPT reaction (*vide infra*) since an abundant amount of negative charge around a proton acceptor is considered to be the driving force for the effective ESIPT reaction in various aromatic compounds.[24-29]

Table 1. Vertical excitation energies (ΔE, kcal/mol), oscillator strengths (*f*), dipole moments (D.M., Debye), and the character of singly occupied orbitals for different transitions of 2-HEAQ·5H_2O calculated at the CASPT2//CASSCF(12e/10o)/6-31G* level of theory. The values in parentheses show ΔE computed at the CASPT2//CASSCF(12e/10o)/6-31G** level of theory.

Transitions	D.M.	*f*	ΔE	Singly occupied orbitals	
S_0	7.7		0.0		
$S_0\rightarrow S_{NP}(^1n\pi^*)$	9.4	0.0004	66.2	n	π*
$S_0\rightarrow S_{LCT1}(^1\pi\pi^*)$	4.2	0.0259	84.1(84.1)	π_{L1}	π*
$S_0\rightarrow S_{LCT2}(^1\pi\pi^*)$	10.7	0.0724	88.4(88.5)	π_{L2}	π*
$S_0\rightarrow S_{RCT1}(^1\pi\pi^*)$	6.9	0.3527	89.6(89.7)	π_{R1}	π*
$S_0\rightarrow S_{RCT2}(^1\pi\pi^*)$	9.5	0.3699	109.7(109.8)	π_{R2}	π*

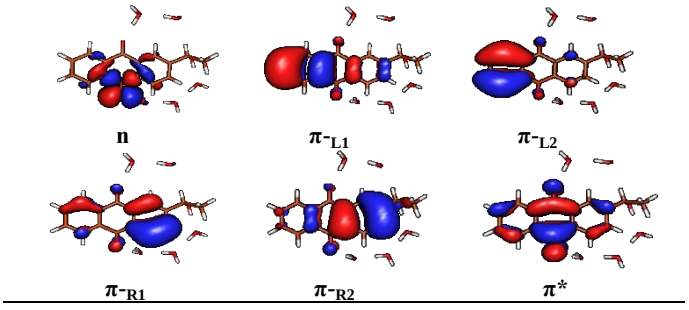

Similar to the $S_0 \rightarrow S_{RCT1}(^1\pi\pi^*)$ and $S_0 \rightarrow S_{RCT2}(^1\pi\pi^*)$ transitions, electron promotion can also be triggered initially from the two degenerate π orbitals with two nodes on the left chromophore, i.e., the unsubstituted benzene ring, to the π* orbitals located on the two C=O groups, which produces another pair of excited states, referred to as $S_{LCT1}(^1\pi\pi^*)$ and $S_{LCT2}(^1\pi\pi^*)$. The approximately isoenergetic FC excitation with CT character for these two transitions was further confirmed by the CASPT2//CASSCF(12e/10o)/6-31G* (84.1 vs. 88.4 kcal/mol) and CASPT2//CASSCF(12e/10o)/6-31G** (84.1 vs. 88.5 kcal/mol) computations. In contrast, the energy splitting between the $S_0 \rightarrow S_{RCT1}(^1\pi\pi^*)$ and $S_0 \rightarrow S_{RCT2}(^1\pi\pi^*)$ transitions significantly increases to ca. 20.0 kcal/mol for the excitation of the right chromophore when the 1'-hydroxyethyl group is introduced in the C2 position on the right benzene ring. This result is primarily due to the electron-withdrawing effect of the 1'-hydroxyethyl group, which prohibits the electron transfer from the 1-phenylethanol group to the two C=O groups in the $S_0 \rightarrow S_{RCT2}(^1\pi\pi^*)$ transition. Therefore, a considerable improvement in the energy level of the vertical excitation of the $S_0 \rightarrow S_{RCT2}(^1\pi\pi^*)$ transition was observed compared to those of the $S_0 \rightarrow S_{LCT1}(^1\pi\pi^*)$ and $S_0 \rightarrow S_{LCT2}(^1\pi\pi^*)$ transitions, which originate from the excitation of the unsubstituted left benzene ring. As shown in Table 1, exactly one node appears in the C2 position of the π orbital located in the 1-phenylethanol chromophore for the $S_0 \rightarrow S_{RCT1}(^1\pi\pi^*)$ transition, which indicates that the excited electron is unlikely to appear around the C2 position in the $S_0 \rightarrow S_{RCT1}(^1\pi\pi^*)$ transition. Therefore, hydroxyethyl substitution in C2 position imposes a negligible influence on the $S_0 \rightarrow S_{RCT1}(^1\pi\pi^*)$ transition. The vertical energy of $S_0 \rightarrow S_{RCT1}(^1\pi\pi^*)$ excitation was calculated to be ~89 kcal/mol that is very close to those of the unsubstituted ring-localized excitations [i.e., $S_0 \rightarrow S_{LCT1}(^1\pi\pi^*)$ and $S_{LCT2}(^1\pi\pi^*)$]. In contrast, the $S_0 \rightarrow S_{RCT2}(^1\pi\pi^*)$ vertical excitation energy was calculated to be 109.0~110.0 kcal/mol, indicating an improvement compared to the three types of excitation mentioned above. This computed excitation energy for the "bright" $S_{RCT2}(^1\pi\pi^*)$ excitation is consistent with the experimental wavelength of 266 nm (107.4 kcal/mol),[23] which was obtained using transient absorption and time-resolved resonance Raman spectroscopy techniques.[23] It can be concluded that the $S_0 \rightarrow S_{RCT2}(^1\pi\pi^*)$ transition is responsible for the initial population under the high-energy excitation experimental conditions.

The vertical excitation energy for the lowest "dark" spectroscopic state [i.e., $S_0 \rightarrow S_{NP}(^1n\pi^*)$] was 66.2 kcal/mol, which is very close to the experimentally observed absorption band at 424 nm (67.4 kcal/mol) for the n→π* transition.[20] This energy is 15~27 kcal/mol lower than those for compounds containing a benzoyl chromophore, such as BP[24] (93.7 kcal/mol), *o*-acetylphenylacetic acid[25] (81.2 kcal/mol) and KP[26] (93.5 kcal/mol). This low energy level for the FC excitation was also found for the π→π* transitions of AQ compared to the corresponding excitations in *o*-acetylphenylacetic acid, KP and BP.[24-26] The ring-closing between the two benzene rings of AQ leads to an increase in the conjugated chain compared to those of benzoyl compounds, which stabilizes the lowest-lying unoccupied π* orbital that is an electron acceptor for the different transitions in AQ and accounts for the low energy excitation of different n/π→π* transitions. Therefore, the photoredox reaction for AQ compounds is able to occur under mild reaction conditions based on an energetic perspective.

Nonadiabatic Decay followed by the ESIPT reaction in the Charge Transfer Triplet State

Figure 1 shows the schematic MEP for the nonadiabatic decay of 2-HEAQ·5H_2O followed by the first step of ESIPT between the 1'-substituted hydroxyl (O13-H14) and carbonyl C10=O12 in the triplet state. The CASSCF(12e/10o)/6-31G* optimized structures for 2-HEAQ·5H_2O in the S_0, S_{RCT2} ($^1\pi\pi^*$) and T_{RCT2} ($^3\pi\pi^*$) electronic states are schematically shown in Figure S2-1 of the ESI along with selected bond parameters. As shown in

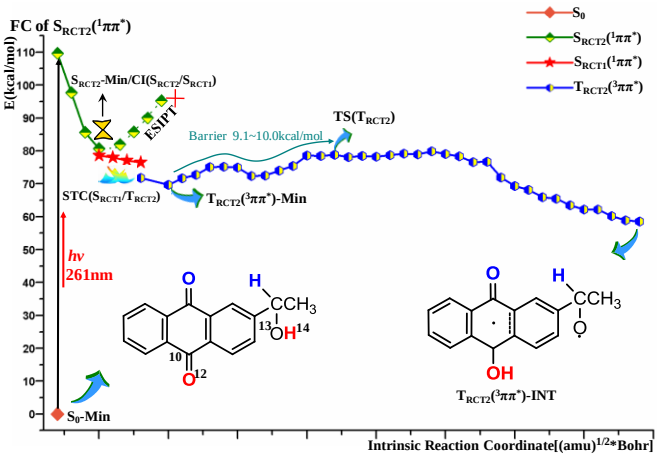

Figure 1. Schematic MEP of ESIPT between 1'-substituted hydroxyl (O13-H14) and carbonyl C10=O12 in the $T_{RCT2}(^3\pi\pi^*)$ state calculated at the CASPT2//IRC/CASSCF(12e/10o)/6-31G* level of theory.

Figure 1, after the initial excitation at 261 nm in the FC of the $S_{RCT2}(^1\pi\pi^*)$ state, 2-HEAQ·5H_2O rapidly decays to its minimum, $S_{RCT2}(^1\pi\pi^*)$-Min, which lies 29.0 kcal/mol below the FC point, via a downhill relaxation path. This initial relaxation is characterized by structural changes where the right benzene ring is enlarged and the C9=O11/C10=O12 bonds become weaker. For example, the C-C bonds in the substituted aromatic ring are elongated to ca. 1.45 Å in $S_{RCT2}(^1\pi\pi^*)$-Min from ~1.40 Å in S_0-Min, and the bond lengths of the two carbonyl groups are slightly increased. This structural adjustment confirms that the initial FC excitation of $S_0 \rightarrow S_{RCT2}(^1\pi\pi^*)$ is associated with the above two moieties in 2-HEAQ with charge translocation along the desired direction. With the minor elongation of the C10=O12 (1.204→1.216 Å) and C9=O11 (1.202→1.212 Å) bonds, the strength of the intramolecular hydrogen bond around the carbonyl group becomes slightly stronger along two water wires in the adiabatic relaxation from FC to the $S_{RCT2}(^1\pi\pi^*)$ minimum. However, these structural changes impose a negligible influence on the strength of the C1′-H15 and O13-H14 bonds, which are the potential proton donors for the ESIPT reaction. As shown in Figure 2, the energy rapidly increases in the $S_{RCT2}(^1\pi\pi^*)$ state and reaches more than 24.0 and 17.0 kcal/mol, respectively, with respect to $S_{RCT2}(^1\pi\pi^*)$-Min when H14/H15 deviates 1.3/1.4 Å from O13/C1′. This result indicates that the deprotonation from the 1'-hydroxyethyl moiety is most likely not initiated in the high-energy $S_{RCT2}(^1\pi\pi^*)$ state. Meanwhile, the protonation reaction of the carbonyl groups (i.e., C9=O11/C10=O12) from the proton donor of the water wires in the $S_{RCT2}(^1\pi\pi^*)$ state are also examined and shown in the MEP of Figure 3. A sizeable barrier (>24.0 kcal/mol) is found when the proton H16 gradually approaches the C10=O12 carbonyl group. All

these computational pieces of evidence indicate that there is a low reactivity in the singlet excited state of $S_{RCT2}(^1\pi\pi^*)$ through the de-protonation and protonation pathways. This is in contrast to the result for BP where the protonation of the carbonyl group in the bright $^1\pi\pi^*$ state occurs smoothly to overcome a tiny barrier.[24] The excessive negative charge photoinitiated by UV light from the substituted benzene ring is distributed to two carbonyl groups and the central ring with the increased conjugation in 2-HEAQ, while the

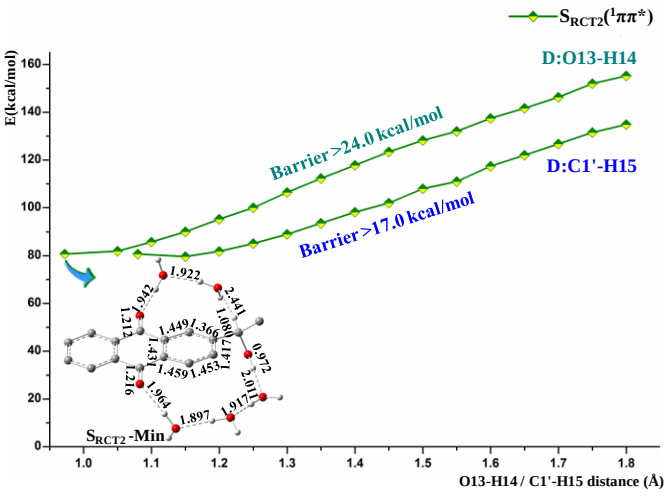

Figure 2. The schematic MEP for the deprotonation of 1'-substituted hydroxyl (O13-H14)/methylene C1'-H15 in the $S_{RCT2}(^1\pi\pi^*)$ state along the reaction coordinate of O13-H14/C1′-H15 distance obtained at the CASPT2//CASSCF(12e/10o)/6-31G* level of theory.

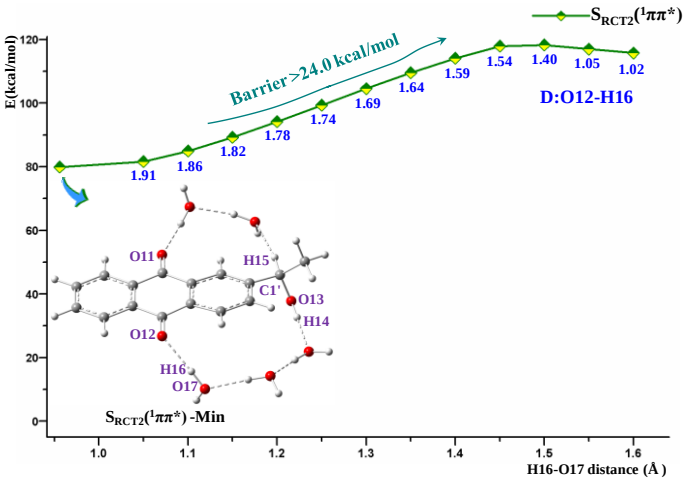

Figure 3. The schematic MEP for the protonation of the carbonyl oxygen O11 in the $S_{RCT2}(^1\pi\pi^*)$ state along the reaction coordinate of H16-O17(or 012-H16, shown in blue) distance obtained at the CASPT2//CASSCF (12e/10o)/6-31G* level of theory.

charge delocalizes along one carbonyl group and the benzoyl chromophore of m-BPOH. Therefore, the carbonyl groups of 2-HEAQ (~0.05) receives a one-fold less excessive negative charge compared to that in m-BPOH (~0.085) in the singlet CT excited state.[24] This result indicates that the carbonyl groups in AQ are poorer proton acceptors than that in BP upon photoinitiated CT along the desired direction in the singlet excited state, which accounts for the high barrier of the deprotonation and protonation reactions in the $S_{RCT2}(^1\pi\pi^*)$ state for 2-HEAQ. These results suggest that the gathering of excessive negative charge around the proton acceptor is a critical condition for the ESIPT reaction and the self-photoredox reaction is unlikely to directly occur in the $S_{RCT2}(^1\pi\pi^*)$ state through an intramolecular proton transfer. Therefore, nonadiabatic relaxation is required to decay the system in lower excited state where energetically accessible channels for the ESIPT reaction must be located which are aided by water wires.

As expected, a conical intersection [$CI(S_{RCT2}/S_{RCT1})$] was determined to join the $S_{RCT2}(^1\pi\pi^*)$ and $S_{RCT1}(^1\pi\pi^*)$ surfaces using the state-averaged CASSCF method with different weights (0.0:0.5:0.5). Closer analyses indicated that there is little difference between $CI(S_{RCT2}/S_{RCT1})$ and $S_{RCT2}(^1\pi\pi^*)$-Min based on the structural features and energy levels, which indicates that $CI(S_{RCT2}/S_{RCT1})$ and $S_{RCT2}(^1\pi\pi^*)$-Min are located in the same region on the MEP. Therefore, the system will be able to effectively decay to the $S_{RCT1}(^1\pi\pi^*)$ state via this funnel. As previously discussed, the $S_0 \rightarrow S_{RCT1}(^1\pi\pi^*)$ excitation is not involved in the substituted hydroxyethyl group that contains the proton donor for the ESIPT reaction. Therefore, $S_{RCT1}(^1\pi\pi^*)$ is unlikely to serve as the precursor state for the self-photoredox process, which is confirmed by the high barrier pathway as the O13-H14 distance increased in the $S_{RCT1}(^1\pi\pi^*)$ state (see the **ESI:** Figure S2-2). On the other hand, the spin-orbital coupling (SOC) between the $S_{RCT1}(^1\pi\pi^*)$ and $T_{RCT2}(^3\pi\pi^*)$ states is found to increase gradually and reaches a maximum (63.5 cm^{-1}) at the critical point of singlet-triplet crossing [$STC(S_{RCT1}/T_{RCT2})$] that is determined to lie 4.2 kcal/mol below $S_{RCT2}(^1\pi\pi^*)$-Min. Such a strong SOC allows for an effective intersystem crossing to occur within ~10.0 ps.[23] This more rapid spin-forbidden process probably originates from the different orbital configurations of the two π orbitals along two mutually perpendicular directions (see Table 1), which is beyond the El-Sayed selection rules[46] and may be ascribed to other factors[47] favoring an effective intersystem crossing between the two ππ* states.

Passing through the nonadiabatic relay of $STC(S_{RCT1}/T_{RCT2})$, the 2-HEAQ system relaxes to the low-lying triplet state minimum (T_{RCT2}-Min) with an adiabatic excitation of 69.7 kcal/mol with respect to the S_0-Min zero level. The vertical excitation energy for the spin-forbidden $S_0 \rightarrow T_{RCT2}(^3\pi\pi^*)$ was determined to be 74.9 kcal/mol (382 nm) with a considerably low oscillator strength. This result is similar to the previous observation of the triplet state absorption at 380 nm.[7(a),22(c),23] In comparison to the singlet-state feature, the striking change is associated with the nature of the singly occupied orbital in the $T_{RCT2}(^3\pi\pi^*)$ state. The reactive moiety of CH_3CHOH gradually becomes involved in the charge transfer from the right chromophore of 1-phenylethanol to the central anthraquinone ring, which is shown in the diagram of the singly occupied orbitals along the $T_{RCT2}(^3\pi\pi^*)$ state reaction pathway in Figure 4. The alternation of the electron population from the singlet to triplet state causes significant changes in the geometric structures of the corresponding minima, as indicated by the structural

adjustment in the substituted benzyl ring with approximately equal C-C bonds (ca. 1.45 Å) in $S_{RCT2}(^1\pi\pi^*)$-Min to the "two short (C3-C4/C1-C16: ~1.35 Å)-four long (other C-C bonds > 1.45 Å)" structural arrangement in T_{RCT2}-Min. These architectural features in the triplet state have been repeatedly observed in many aromatic compounds.[48]

In addition to the structural changes in the substituted benzyl ring, the carbonyl C10=O12 is slightly elongated from 1.216 Å in $S_{RCT2}(^1\pi\pi^*)$-Min to 1.221 Å in T_{RCT2}-Min while the C9=O11 bond shortens from the singlet to the triplet minimum. This indicates that the two carbonyl groups have different reactivity for the subsequent ESIPT in the triplet state and this was further confirmed by the following IRC pathway calculations. As shown in Figure 1 and in the structural evolution along the $T_{RCT2}(^3\pi\pi^*)$ state ESIPT pathway in Figures S2-1 of the **ESI**, the reaction was initially triggered by the departure of proton H14 from 1'-substituted hydroxyl (O13-H14), which instantaneously leads to a series of structural adjustment in the hydrogen bonds along the W1-W2-W3 water wire. Meanwhile, the noticeable elongation was observed for the C1′-O13(H14) and carbonyl C10=O12 bonds, which are the donor and acceptor, respectively, for the ESIPT reaction in the $T_{RCT2}(^3\pi\pi^*)$ state. This result suggests that the deprotonation of the 1'-substituted hydroxyl (O13-H14) and the protonation of the carbonyl C10=O12 by the connecting water molecules proceed in a concerted manner in the lowest triplet state. Since the bond fission gets involved in this reaction, the energy level inevitably increases in the early decay phase of this water assisted ESIPT process. Another favorable factor can be explored to drive the subsequent ESIPT reaction.

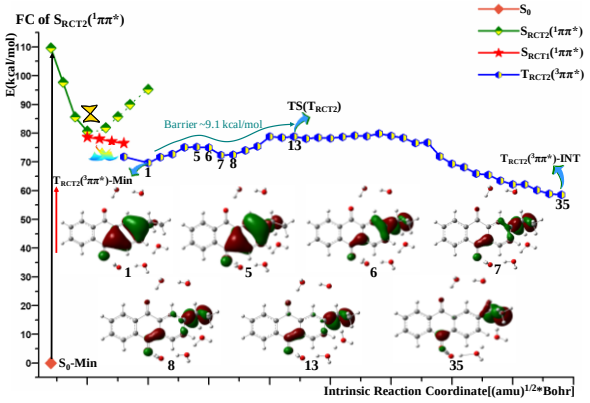

Figure 4. The evolution of the character of the singly occupied orbitals for 2-HEAQ·5H2O are schematically illustrated along the MEP for the first step of ESIPT between the 1'-substituted hydroxyl (O13-H14) and the carbonyl C10=O12 in the $T_{RCT2}(^3\pi\pi^*)$ state.

Fortunately, the CH_3CHOH group gradually takes part in the CT process between the two moieties of 2-HEAQ with the evolution of the water assisted ESIPT reaction, which is confirmed by the alternation of the characteristics of the singly occupied orbitals (see Figure 4). Therefore, the "two short-four long" structural feature in the triplet state disappears until one singly occupied orbital is unambiguously distributed in the reactive moiety of CH_3CHOH, especially in C1'. The donor for the photoinduced charge transfer significantly shifts from the right chromophore in the nonadiabatic relaxation and the initial phase of the triplet state ESIPT to its side chain alcohol CH_3CHOH moiety when the energy level begins to increase. This alternation results in a decrease in electron density around O13, facilitating the departure of proton H14 from O13. Consequently, a broad and flat energy plateau appears near the transition state in the $T_{RCT2}(^3\pi\pi^*)$ state, denoted as $TS(T_{RCT2})$. As shown in Figure S2-1 of the **ESI**, proton H14 has already deviated 1.462 Å from O13 in $TS(T_{RCT2})$, resulting in a strong intermolecular hydrogen bond between proton H14 and W1 (1.065 Å). Meanwhile, the proton of W1 leaves the original position and approaches the second water of W2, which indicates that the proton switching for W1 has been completed in $TS(T_{RCT2})$, triggering the subsequent proton transfer via the relay of W2. Therefore, the proton transfer from the CH_3CHOH group to W1 and then a proton from W1 to W2 and then a proton from W2 to W3 that then transfer a proton to the carbonyl C10=O12 was achieved via the concerted proton switching assisted by the W1-W2 -W3 water wire, which can be observed from the structural evolution in Figure S2-1 of the **ESI**. This indicates that the protonation of the carbonyl group observed in the time-resolved spectroscopy experiments needs the presence of water to take place and that the proton that actually protonates the carbonyl group comes from a water solvent molecule.[23] This is further supported by additional experimental evidence from photochemistry experiments reported by Wan and coworkers in a D_2O solution which showed that the proton for the formation of the O-H(D) from the reduction of the carbonyl group comes from the water solvent and not the molecule itself.[30(b)] The energy consumption of the O-H bond fission is approximately compensated by the simultaneous formation of other O-H bonds along the water wire, which accounts for the existence of the broad energy plateau around $TS(T_{RCT2})$ in the triplet state ESIPT pathway. The $TS(T_{RCT2})$ was calculated to be ca. 9.1~10.0 kcal/mol above the zero level of the T_{RCT2}-Min at both the CASPT2//CASSCF(12e/10o)/6-31G* and CASPT2//CASSCF (12e/10o)/6-31G** level of theory. Considering that the ESIPT reaction takes place in the low-energy triplet state, this moderate barrier enables the triplet ESIPT reaction to occur smoothly aided by a proton migration relay with three water molecules (W1, W2 and W3).

Following a downhill relaxation path, the carbonyl C10=O12 is reduced to its alcohol form due to the formation of the O-H bond to lead to generating the triplet state intermediate of T_{RCT2}-INT. This intermediate has a partially reduced semi-anthraquinone structure in the central ring and is calculated to be 11.2 kcal/mol with respect to the T_{RCT2}-Min zero level. For the T_{RCT2}-INT configuration, a triplet $\rightarrow$ triplet absorption with a low oscillator strength (f=0.017) was energetically calculated to be ~57.2 kcal/mol (500 nm) which is in good agreement with the λ_{max} at 510 nm for the transient weak absorption band observed for the triplet state intermediate that was previously assigned to the intermediate X in the time-resolved spectroscopy experiments.[23]

To further verify the role the water molecule(s), the T_{RCT2} state ESIPT reaction pathways of the isolated 2-HEAQ without the aid of water wires were calculated respectively in the gas phase and in water solution using the polarizable continuum model (see Figure S2-3 and Table S3-5 in the ESI). The proton H14 of $TS(T_{RCT2})$ is almost equidistant from the donor (O13) and acceptor (O12) of the ESIPT reaction in the T_{RCT2} state for the isolated 2-HEAQ. The energy maximum shows a large deviation distance (>4.0 Å) between

the proton H14 and its acceptor carbonyl C10=O12, indicating an extremely weak interaction between O12 and H14 in comparison with the case of 2-HEAQ·5H_2O in the T_{RCT2} state ESIPT reaction. This means that the attraction role caused by the negative charge center of the carbonyl C10=O12 can't effectively impose on the transferred proton (H14) through such a large spatial distance without the aid of the water solution media (i.e., water wire). As can be expected, sizeable barriers were determined for the isolated 2-HEAQ triplet state ESIPT reaction in the gas phase and in the polar water solution that only considered a polarizable continuum model for water (ca. 50.0 kcal/mol). With respect to the zero level of S_0, these barriers are > 110.0 kcal/mol and approximately equal to the fission energy of an O-H bond. This indicates that photoexcitation does not lead to any favourable influence on the ESIPT reaction without the explicit assistance of the water media. These computational results reveal that the ESIPT reaction is unlikely to take place in the T_{RCT2} state in the absence of a water wire. Therefore, the water molecules function as an effective proton relay to lower the ESIPT reaction barrier. The polar surrounding solvent imposed by the water solution only perturbs the reaction barrier to some extent but does not fundamentally modify the reaction mechanism. Consistently, experimental studies show that the participation of water molecule is a precondition for the occurrence of the photoredox reaction.[23] Moreover, isotopic labeling experiments conducted in D_2O solution by Wan and coworkers reveal that the reduction of the carbonyl group comes from the water solvent.[30(b)]

We should note several things from the preceding discussion of the theoretical results and their relationship to several experimental observations. First, the presence of water (whether in a neutral or acidic environment) is needed for the protonation of the carbonyl group that is part of the novel photoredox chemistry observed in some *meta* substituted AQ and BP derivatives.[22-23] This is consistent with experimental photochemical and time-resolved spectroscopy results that show the photoredox reactions of interest only occur appreciably in the presence of water.[22-23] Second, the water molecules facilitates a connection that allows a process or "communication" between the *meta* substituted CH_3CHOH group and the distal carbonyl group that leads to protonation of this carbonyl group by the water molecule hydrogen bonded to it. This is one of the key ingredients for the photoredox reaction to be able to take place at distal groups on the *meta* substituted AQ and BP compounds that exhibit efficient photoredox reactions.[22-23] This proton transfer aided by the relay of water wire or "communication" process is what enables and drives the water that is hydrogen bonded to the carbonyl group to be able to protonate this carbonyl group. This is consistent with and in agreement with the time-resolved experimental observation of the triplet state of AQ (intermediate A with transient absorption bands at 381 nm and 454 nm) being protonated at a carbonyl group to produce the triplet state intermediate of T_{RCT2}-INT (which is the intermediate X with transient absorption bands at 395 nm and 510 nm in reference 23) and also the photochemistry results of Wan and coworkers in a D_2O solution which demonstrate the proton comes from the water solvent molecules and not the molecule itself.[23,30(b)]

Self-photoredox of Semi-Anthraquinone through the ESIPT Reaction Aided by a Water Wire in the Triplet and Ground States

As shown in Figures 5, T_{RCT2}-INT exhibits a typical diradical configuration in which two unpaired electrons are distributed around O13 and the central ring and especially in carbonyl C9=O11. The electronic configuration of the diradical leads to an extremely long C1'-O13 bond in T_{RCT2}-INT (1.442 Å) compared to that in S_0-Min (1.401 Å). This unstable moiety tends to lose proton H15 through a deprotonation reaction that is able to trigger another ESIPT reaction assisted by a short water wire (W4-W5). As shown in Figure 5, the energy level undergoes a minor increase when the proton H15 deviates from C1'. Consequently, a small barrier (ca. 5.7 kcal/mol)

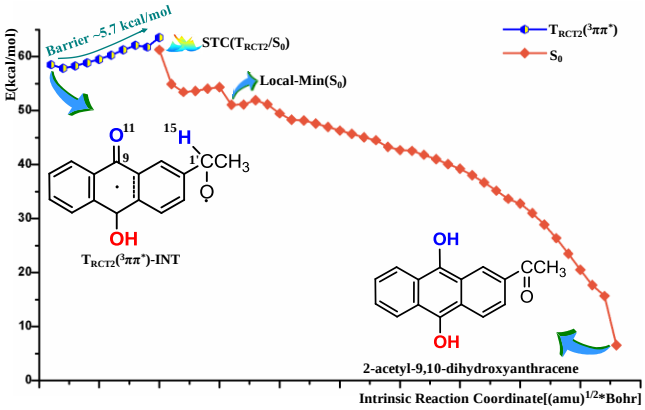

Figure 5. Schematic MEPs of the deprotonation reaction from methylene C1'-H15 in the $T_{RCT2}(^3\pi\pi^*)$ state followed by the protonation of carbonyl oxygen O11 in the ground state calculated at the CASPT2//IRC/CASSCF(12e/10o)/6-31G* level of theory.

above the zero level of T_{RCT2}-INT is encountered when the C1'-H15 bond elongates to 1.156 Å from 1.083 Å in this triplet intermediate. The departure of proton H15 significantly strengthens the C1'-O13 bond from 1.442 Å in T_{RCT2}-INT to 1.334 Å in the critical point of the energy maximum. The results from the CASPT2 computations indicate that this energetic maximum corresponds to the singlet-triplet crossing between the $T_{RCT2}(^3\pi\pi^*)$ and the ground states and therefore, this maximum is referred to as STC(T_{RCT2}/S_0). This energetically degenerate state functions as an effective nonadiabatic relay to bring the system down to the ground state surface. The initial deprotonation of the H15 in the ground state proceeds smoothly along a downhill energy pathway. A local minimum, denoted as Local-min(S_0), was determined to locate 10.2 kcal/mol below STC(T_{RCT2}/S_0) when proton H15 is equidistant (1.434 vs. 1.411 Å) between C1' and the water molecule of W4. Meanwhile, the C1'-O13 bond is further shortened to 1.273 Å and some double bond character begins to develop. The singlet → singlet absorption of Local-min was energetically calculated to be ~50.0 kcal/mol (564 nm).

Structural comparisons among T_{RCT2}-INT, STC(T_{RCT2}/S_0) and Local-min(S_0) indicate that there are minor changes in the carbonyl C9=O11 along with the W4-W5 water wire even though the deprotonation reaction in CH_3CHOH portion is nearly completed.

This behavior is different from the previous photoredox reaction between carbonyl C10=O12 and hydroxy O13-H14 via a water wire where the deprotonation and protonation reactions proceed in a concerted manner. However, the protonation of the carbonyl C9=O11 was not triggered in the early phase of the C1'-H15 deprotonation, suggesting a non-concerted mechanism for the second step of the redox reaction. As shown in Figure 5, the rest of the reaction after Local-min(S_0) occurs easily along a sharply decreasing energy pathway. The movement of the proton H15 triggers the subsequent two-step proton switching via a proton migration relay (W4 and W5) that transforms the carbonyl C9=O11 to its reduced state (i.e., alcohol). In addition, the departure of H15 results in the continuous shortening of the C1'-O13 bond to a normal carbonyl bond (1.217 Å) which results in an oxidized CH_3CHOH moiety. Meanwhile, the double bond positions undergo alternation throughout the whole aromatic ring, eventually producing the final self-photoredox product (i.e., 2-acetyl-9,10-dihydroxyanthracene), which is 6.5 kcal/mol less stable than the starting reactant at the ground state minimum (S_0-Min).

The preceding theoretical non-concerted step-wise process with the first step being deprotonation is consistent with the experimental time-resolved experiments that showed the triplet state intermediate of T_{RCT2}-INT (which is the intermediate X with transient absorption bands at 395 nm and 510 nm in reference 23) next evolving into an intermediate B (Local-min in the ground state) with transient absorption bands at 392 nm and 600 nm in reference 23 and then this intermediate was experimentally observed to then produce the product, 2-acetyl-9,10-dihydroxyanthracene which is the species C with absorption bands at 370 nm and 480 nm (calculated wavelength, 454 nm) observed in the time-resolved spectra of reference 23. The last step of this theoretical nonconcerted photoredox process indicates that the protonation of the semi-quinone group carbonyl group is done by the water molecule hydrogen bonded to it and this is consistent with the experimental photochemistry results of Wan and coworkers done in D_2O solutions that indicate that water is the source of the proton that protonates this carbonyl.[30(b)] It is interesting that this non-concerted process starts with a deprotonation that is asynchronously linked by water molecules to the protonation of the other carbonyl of the semi-anthraquinone part of the system which leads to the oxidation of the *meta*-substituted side chain of CH_3CHOH to transform its alcohol to a carbonyl and through the water connecting molecules enable the protonation of the carbonyl C9=O11 on the semi-anthraquinone group to reduce this carbonyl to its alcohol and thus end up producing the product, 2-acetyl-9,10-dihydroxyanthracene. Both the concerted and non-concerted photoredox processes use water molecules to connect the deprotonation and protonation processes. However, there appears to be appreciable flexibility in the connecting water molecules ability to "communicate" the deprotonation-protonation process at distal sites in a molecule so that it can appear to be either a fast synchronous concerted process which accounts for the experimental transformation of the triplet state of AQ (intermediate A with transient absorption bands at 381 nm and 454 nm) being protonated at a carbonyl group to produce the triplet state intermediate of T_{RCT2}-INT (which is the intermediate X with transient absorption bands at 395 nm and 510 nm in reference 23) or be a slower asynchronous step-wise process that accounts for the experimentally observed transformation of this intermediate into an intermediate B with transient absorption bands at 392 nm and 600 nm in reference 23 and then this undergoes subsequent reaction to form the product, 2-acetyl-9,10-dihydroxyanthracene which is the species C with absorption bands at 370 nm and 480 nm observed in the time-resolved spectra of reference 23. For the non-concerted photoredox process, it is interesting that the deprotonation at the side chain to oxidize the alcohol to a carbonyl is almost complete but the water molecules connection still facilitates the protonation of the distal carbonyl group of the semi-anthraquinone group to produce an alcohol and enable formation of the final product. It will be interesting to do further experiments to see what factors will influence these types of photoredox reactions that are essentially deprotonation-protonation at distal parts of a molecule facilitated by water (and/or acid) molecules connecting these photoredox sites. Our results here in combination with the experimental results reported previously by Wan and coworkers[22] and Phillips and coworkers[23] suggest that it may be worthwhile to examine how water and/or acid assisted deprotonation-protonation coupled processes may take place in larger molecules and systems to accomplish photoredox or other related reactions.

Conclusions

In this study, multi-configurational second-order perturbation theory has been employed to investigate a novel self-photoredox reaction for anthraquinone. As shown in Scheme 2, photoexcitation at ~261 nm induces charge transfer along the desired direction from the right chromophore (i.e. the substituted ring) to the central ring, especially the two carbonyl groups, which promotes the system to populate the $S_{RCT2}(^1\pi\pi^*)$ excited state. From this state, it is very easy to relax to the$T_{RCT2}(^3\pi\pi^*)$ state via an effective singlet−triplet crossing that is regulated by the intermediate state of $S_{RCT1}(^1\pi\pi^*)$. Following the nonadiabatic decay, a moderate barrier (9.1~10.0 kcal/mol) is overcome to initiate the triplet state ESIPT reaction assisted by a water wire, allowing for simultaneous deprotonation of the side chain alcohol moiety and pronation of one carbonyl group in the central ring by a nearby water molecule. Aided by the water wire, the substituted 1'-hydroxyethyl group gradually takes part in the photoinitiated charge transfer along the desired direction in the later phase of this water assisted ESIPT process, which plays a decisive role in lowering the reaction barrier and allowing for the formation of the diradical intermediate in the triplet state. After overcoming a small barrier (5.7 kcal/mol) through the deprontonation of C-H in the $^3\pi\pi^*$ CT state, the diradical intermediate relaxes to the singlet−triplet crossing of STC(T/S_0), which allows an efficient spin-forbidden decay to the ground state. The subsequent protonation reaction of another carbonyl group proceeds smoothly along a downhill energy pathway through proton switching aided by a water wire to yield the final product for the self-photoredox of

anthraquinone. Compared with the case of *m*-BPOH, the carbonyl groups of 2-HEAQ receive a one-fold less excessive negative charge upon photoinitiated CT along the desired direction in the singlet excited state. This explains the reason why high barriers were found along the reaction pathways of the deprotonation and protonation in the singlet excited state for 2-HEAQ. As an important consequence, the self-photoredox reaction takes place in the CT triplet state through an enhanced spin-orbital coupling in the region of the singlet-triplet crossing. The present computational efforts together with our previous results[24-29] provide benchmarks for understanding the water-assisted ESIPT mechanism of AQ and BP, as well as their analogous compounds in aqueous solutions.

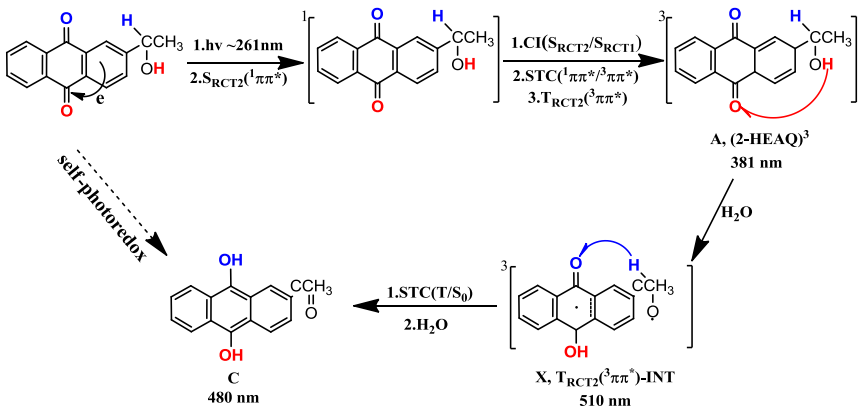

Scheme 2. Plausible Mechanism for the Water-Assisted Self-Photoredox of 2-(1-Hydroxyethyl)-9,10-Anthraquinone Proposed by Theoretical Simulations using ab initio Multi-configurational Perturbation Theory.

Acknowledgements

This work has been supported by the grants NSFC21373029 (X.C.), 2011CB808503 (W.F.) and the Research Grants Council of Hong Kong (HKU 17301815) to DLP.

References

1 J. M. Bruce in *The Chemistry of the Quinoide Compounds* (Ed.: S. Patei), Wiley, New York, 1974, pp. 465–538.
2 H. Gan, D. G. Whitten, *J. Am. Chem. Soc.* 1993, **115**, 8031–8037.
3 S. A. Carlson, D. M. Hercules, *Photochem. Photobiol.* 1973, **17**, 123–131.
4 M. Shah, N. S. Allen, M. Edge, S. Navaratnam, F. Catalina, *J. Appl. Polymer Sci*. 1996, **62**, 319–340.
5 I. Loeff, A. Treinin, H. Linschitz, *J. Phys. Chem.* 1983, **87**, 2536–2544.
6 F. *J*. Wilkinson, *Phys. Chem*. 1962, **66**, 2569–2574.
7 a) H. Görner, *Photochem. Photobiol.* 2003, **77**, 171–179; b) H. Görner, *Photochem. Photobiol. Sci.* 2004, **3**, 933–938; c) H. Görner, *Photochem. Photobiol. Sci*. 2006, **5**, 1052–1058.
8 a) N. S. Allen, G. Pullen, M. Shah, M. Edge, I. Weddell, R. Swart, F. Catalina, *Polymer*. 1995, **36**, 4665; b) N. S. Allen, J. F. McKellar, *in Ueoelopments in Polymer Photochemistry*. 1980, 191; c) N. S. Allen, J. F. McKellar, *Photochemistry of Dyed and Pigmented Polymers*. 1980.
9 A. N. Diaz, *J. Photochem. Photobiol. A*: *Chem*. 1990, **53**, 141.
10 a) T. Furuta, Y. Hirayama, M. Iwamura, *Org. Lett*. 2001, **3**, 1809−1812; b) T. Furuta, H. Torigai, M. Sugimoto, M. Iwamura, *J. Org. Chem*. 1995, **60**, 3953−3956.
11 M. G. Ren, N. M. Bi, M. Mao, Q. H. Song, *J. Photochem. Photobiol. A*: *Chem*. 2009, **204**, 13−18.
12 a) R. G. Brinson, P. B. Jones, *Org. Lett.* 2004, **6**, 3767−3770; b) R. G. Brinson, S. C. Hubbard, D. R. Zuidema, P. B. Jones, *J. Photochem. Photobiol. A*: *Chem.* 2005, **175**, 118−128; c) P. B. Jones, R. G. Brinson, S. J. Sarma, S. Elkazaz, *Org. Biomol. Chem*. 2008, **6**, 4203−4211.
13 S. J. Sarma, P. B. Jones, *J. Org. Chem.* 2010, **75**, 3806−3813.
14 T. Yoshihara, M. Yamaji, T. Itoh, J. Nishimura, H. Shizuka, S. *J*. Tobita, *Photochem. Photobiol. A*: *Chem*. 2001, **140**, 7–13.
15 A. M. Aquino, C. J. Abelt, K. L. Berger, C. M. Darragh, S. E. Kelley, M. V. Cossette, *J. Am. Chem. Soc*. 1990, **112**, 5819–5824.
16 H. Langhals, S. Saulich, *Chem. Eur. J*. 2002, **8**, 5630–5643.
17 L. Zhu, R. F. Khairutdinov, J. L. Cape, J. K. Hurst, *J. Am. Chem. Soc*. 2005, **128**, 825–835.
18 V. Maurino, D. Borghesi, D. Vione, C. Minero, *Photochem. Photobiol. Sci*. 2008, **7**, 321–327.
19 A. Gouloumis, D. Gonzalez-Rodriguez, P. Vazquez, T. Torres, S. Liu, L. Echegoyen, J.; Hug, G. L. Ramey, D. M. Guldi, *J. Am. Chem. Soc*. 2006, **128**, 12674–12684.
20 K. E. Drabe, H. Veenvliet, D. A. Wiersma, *Chem. Phys. Lett*. 1975, **35**, 469–474.
21 K. Maruyama, A. Osuka, *The Chemistry of the Quinoide Compounds* (Eds.: S. Patei, Z. Rappaport), Wiley, New York, 1988, pp. 737–878.
22 a) M. Lukeman, M. S. Xu, P. Wan, *Chem. Commun.* 2002, **2**, 136–137; b) Y. Y. Hou, P. Wan, *Photochem. Photobiol. Sci.* 2008, **7**, 588–596; c) Y. Hou, L. A. Huck, P. Wan, *Photochem. Photobiol. Sci*. 2009, **8**, 1408−1415.
23 J. Ma, T. Su, M. D. Li, L. W. Du, J. Q. Huang, X. G. Guan, D. L. Phillips, *J. Am. Chem. Soc.* 2012, **134**, 14858−14868.
24 X. B. Chen, Q. Q. Zhang, Y. C. Xu, W. H. Fang, D. L. Phillips, *J. Org. Chem*. 2013, **78**, 5677−5684.
25 L. N. Ding, X. B. Chen, W. H. Fang, *Org. Lett*. 2009, **11**, 1495 –1498.
26 Y. C. Xu, X. B. Chen, W. H. Fang, D. L. Phillips, *Org. Lett.* 2011, **13**, 5472−5475.
27 L. Ding, L. Shen, X. B. Chen, W. H. Fang, *J. Org. Chem.* 2009, **74**, 8956-8962.
28 X. B. Chen, C. S. Ma, D. L. Phillips, W. H. Fang, *Org. Lett.* 2010, **12**, 5108-5111.
29 L. Ding, W. H. Fang, *J. Org. Chem.* 2010, **75**, 1630-1636.
30 a) L. A. Huck, P. Wan, *Org. Lett*. 2004, **6**, 1797−1799; b) M. Devin, M. Lukeman, L. Dan, P. Wan, *Org. Lett*. 2005, **7**, 3387-3389; (c) N. Basarić, D. Mitchell, P. Wan, *Can. J. Chem*. 2007, **85**, 561−571; d) J. Ma, M. D. Li, D. L. Phillips, P. Wan, *J. Org. Chem*. 2011, **76**, 3710−3719.
31 M. Sobczak, P. J. Wagner, *Org. Lett*. 2002, **4**, 379–382.
32 L. J. Martinez, J. C. Scaiano, *J. Am. Chem. Soc.* 1997, **119**, 11066–11070.

33 M. D. Li, Y. Du, Y. P. Chuang, J. Xue, D. L. Phillips, *Phys. Chem. Chem. Phys*. 2010, **12**, 4800–4808.
34 M. D. Li, C. S. Yeung, X. G. Guan, J. Ma, W. Li, C. S. Ma, D. L. Phillips, *Chem. Eur. J*. 2011, **17**, 10935–10950.
35 M. D. Li, J. Ma, T. Su, M. Y. Liu, L. H. Yu, D. L. Phillips, *J. Phys. Chem. B* 2012, **116**, 5882−5887.
36 H. J. Wang, X. B. Chen, W. H. Fang, *Phys. Chem. Chem. Phys.* 2014, **16**, 25432-25441.
37 B. O. Roos, P. R. Taylor, P. E. M. Siegbahn, *Chem. Phys*. 1980, **48**, 157.
38 K. Ruedenberg, M. Schmidt, M. M. Gilbert, S. T. Elbert, *Chem. Phys*. 1982, **71**, 41−49.
39 H. J. Werner, P. J. Knowles, *J. Chem. Phys*. 1985, *82*, 5053−5063.
40 K. Fukui, *Acc. Chem. Res.* 1981, **14**, 363–368.
41 H, P. Hratchian, H, B. Schlegel, *J. Chem. Phys*. 2004, **12**, 9918–9924.
42 K. Andersson, P. Å. Malmqvist, B. O. Roos, A. J. Sadlej, K. Wolinski, *J. Phys. Chem*. 1990, **94**, 5483−5488.
43 K. Andersson, P. Å. Malmqvist, B. O. Roos, *J. Chem. Phys*. 1992, **96**, 1218−1226.
44 M. J. Frisch, G. W. Trucks, H. B. Schlegel, G. E. Scuseria, M. A. Robb, J. R. Cheeseman, J. A. Montgomery Jr., T. Vreven, K. N. Kudin, J. C. Burant, J. M. Millam, S. S. Iyengar, J. Tomasi, V. Barone, B. Mennucci, M. Cossi, G. Scalmani, N. Rega, G. A. Petersson, H. Nakatsuji, M. Hada, M. Ehara, K. Toyota, R. Fukuda, J. Hasegawa, M. Ishida, T. Nakajima, Y. Honda, O. Kitao, H. Nakai, M.; Li, X. Klene, J. E. Knox, H. P. Hratchian, J. B. Cross, C. Adamo, J. Jaramillo, R. Gomperts, R. E. Stratmann, O. Yazyev, A. J. Austin, R. Cammi, C. Pomelli, J. W. Ochterski, P. Y. Ayala, K. Morokuma, G. A. Voth, P. Salvador, J. J. Dannenberg, V. G. Zakrzewski, S. Dapprich, A. D. Daniels, M. C. Strain, O. Farkas, D. K. Malick, A. D. Rabuck, K. Raghavachari, J. B. Foresman, J. V. Ortiz, Q. Cui, A. G. Baboul, S. Clifford, J. Cioslowski, B. B. Stefanov, G. Liu, A. Liashenko, P. Piskorz, I. Komaromi, R. L. Martin, D. J. Fox, T. Keith, M. A. Al-Laham, C. Y. Peng, A. Nanayakkara, M. Challacombe, P. M. W. Gill, B. Johnson, W. Chen, M. W. Wong, C. González, J. A. Pople, *Gaussian03 Revision D.02*, Gaussian, Inc. Pittsburgh, PA, 2004.
45 K. Andersson, F. Aquilante, M. Barysz, E. Bednarz, A. Bernhardsson, M. R .A. Blomberg, Y. Carissan, D. L. Cooper, M. Cossi, A. Devarajan, L. De Vico, N. Ferré, M. P. Fülscher, A. Gaenko, L. , Ghigo, G. Gagliardi, C. de Graaf, B. A. Hess, D. Hagberg, A. Holt, G. Karlström, J. W. Krogh, R. Lindh, P.-Å. Malmqvist, T. Nakajima, P. Neogrády, J. Olsen, T. B. Pedersen, J. Raab, M. Reiher, B. O. Roos, U. Ryde, B. Schimmelpfennig, M. Schütz, L. Seijo, L. Serrano-Andrés, P. E. M. Siegbahn, J. Stålring, T. Thorsteinsson, V. Veryazov, P.-O. A. Wolf, *Molcas Version 7.6*, Lund University, Sweden, 2010.
46 a) M. A. El-Sayed, *Acc. Chem. Res.* 1968, *1*, 8-16l; b) M. A. El-Sayed, *J. Chem. Phys*. 1963, **38**, 2834.
47 R. A. Caldwell, *Pure Appl. Chem.* 1984, **56**, 1167.
48 a) X. B. Chen, W. H. Fang, *J. Am. Chem. Soc*. 2004, **126**, 8976−8980; b) W. H. Fang, *Acc. Chem. Res*. 2008, **41**, 452−457.

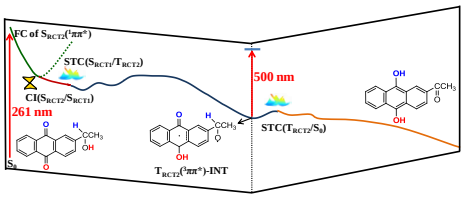

Graphical abstract

A novel self-photoredox reaction for 2-(1-hydroxyethyl)-9,10-anthraquinone has been theoretically rationalized to take place through two steps of triplet excited state intra-molecular proton transfer aided by water wires.